Int. J. Electrochem. Sci., 11 **(2016)** 9206 – 9215, doi: 10.20964/2016.11.23

International Journal of
ELECTROCHEMICAL
SCIENCE
www.electrochemsci.org

Short Communication

Electrodeposition of Super-Hydrophobic Nickel Film on Magnesium Alloy AZ31 and Its Corrosion Resistance

Baojun Han[1,2,*], *Yang Yang*[2], *Ling Fang*[1,2], *Guanghuai Peng*[1,2], *Chubin Yang*[1,2]

[1] Jiangxi Provincial Engineering Research Center for Magnesium alloys, GanNan Normal University, Ganzhou 341000, PR China
[2] School of Chemistry and Chemical Engineering, GanNan Normal University, Ganzhou 341000, PR China
[*]E-mail: bao77junhan@yahoo.com

Received: 30 July 2016 / *Accepted:* 9 September 2016 / *Published:* 10 October 2016

Super-hydrophobic surface has been widely studied owing to its various distinct functions. The original microstructures of the characteristic plant leaves, which are super-hydrophobic, have inspired researchers to design and manufacture synthetic super-hydrophobic surface. Among all the structural-metal materials, magnesium alloy, which is the lightest alloy, was restricted because of its low resistance to erosion. Through the nickel electrodeposition approach, a super-hydrophobic surface, which possess self-cleaning feature, was succeeded to be deposited on AZ31 Mg alloy. To study the wettability of the nickel film, which is super-hydrophobic, the surface was exposed under air ambient at room temperature, where the water contact angle is 151.7°. Moreover, electrochemical impedance spectroscopy (EIS) and Tafel polarization measurements were employed to evaluate the erosion resistance of the super-hydrophobic surface.

Keywords: Electrodeposition, Nickel, Magnesium alloy; EIS, Corrosion; Potentiodynamic polarization

1. INTRODUCTION

Mg alloys, which possess remarkable mechanical and physical properties including high strength/weight ratio, low density, excellent electromagnetic shielding and metal cutting capacity [1, 2]. Consequently, Mg alloys have been exploited in various applications including biological materials[3, 4], aircraft, functional materials, computer industry and etc. [5-9]. However, Mg alloy could be oxidized and corroded easily, as the standard potential of Mg alloy is very low. Thus, numerous applications of Mg alloy are restricted [10, 11].

Recently, super-hydrophobic surfaces have attracted intensive interest in fundamental research as well as their potential applications when their water contact angle (CA) is larger than 150^o and sliding angle (SA) is lower than 10^o, because of their special properties including self-cleaning [12], anti-erosion[13-15], hydrophobicity [16-18] and freeze-proofing property [19-22]. Super-hydrophobic has been demonstrated that they could be manufactured through producing the micro-nanostructured hydrophobic surface or the chemical modification of the micro-nanostructured surface with these materials which have low surface energy [23-26]. By far, numerous methods, such as have plasma-etching [27], anodizing [28-30], chemical vapor deposition [31], sol–gel process [32-34], phase segregation[35] and electrolytic deposition [24, 36], has succeeded to be exploited to fabricate synthetic super-hydrophobic surfaces. However, their real applications have been limited as majority of these approaches require expensive materials or harsh conditions. Moreover, organics have been utilized in these methods to modify the surfaces to decrease the surface energy. However, the surfaces after modification are unstable and easy to be contaminated [37-40]. Thus, an increasing number of tries has been endowed to produce super-hydrophobic surfaces in absence of the materials which has low surface energy. For instance, super-hydrophobic copper surfaces which is lotus-like have been synthesized by electroplating under high current density. Hierarchically nanostructured CuO surface was synthesized by Wang et al. [41] through electrodeposition. The original CuO surface which is super-hydrophilic transformed to be super-hydrophobic when being exposed under air ambient at room temperature for 3 weeks, where the change of the wettability is attributed to the adsorption of oxygen molecules on the top lay of the CuO surface. A surface, which exhibited super-hydrophilic feature just after preparation, was produced by Hang et al. [36] with nickel micro-nano cone array through two steps of electrodeposition. Moreover, the transformation to super-hydrophobicity from super-hydrophilicity when exposing the surface under air ambient for 15 days was reported, which could be ascribed to the change of surface chemical composition as well as the formation of NiO on the surface of Nickel [42]. In order to promote the resistance of super-hydrophobic surfaces to mechanical arrosion, environmental pollution and proper shear stress [43, 44], several processes have been developed.

Nickel is a basic material in engineering and features with various remarkable properties including magnetism, corrosion resistance and high hardness. Thus, Cu could be prevented from erosion by Ni when depositing Ni on the surface of copper. In consideration of its super-hydrophobicity, it is demonstrated that the distinct benefit of nickel coating could expand its applications significantly including anti-pollution and anti-erosion materials. Nevertheless, only a little attention has been attracted to study the properties of super-hydrophobic surfaces including the long-term stability and corrosion resistance, whereas most of efforts have been endowed to produce metallic super-hydrophobic structures in the absence of materials which have low surface energy. Herein, we deposited the AZ31 Mg alloy on the super-hydrophobic films through electrodeposition. Moreover, the polarization and impedance spectroscopy were employed to investigate the corrosion performance of Ni coatings which are super-hydrophobic.

2. EXPERIMENTAL

2.1. Electrodeposition of a super-hydrophobic surface on magnesium alloy AZ31

Mg alloy AZ31 was employed here as a substrate, where the size is 10 mm×10 mm×1.5 mm and the composition is 0.0027% Fe, 0.002% Ni, 0.001% Cu, 0.0135% Si, 0.38% Mn, 0.88% Zn, 2.98% Al and the rest is Mg. Then, the nickel coatings were deposited on the surface of AZ31 substrate by electrodeposition with a direct current. Noted that the substrate was mechanically polished to 4000 grit grade first with rough SiC papers and then by 0.3 mm alumina in prior to plating. Subsequently, the samples were first immersed in acetone for 15 min under ultrasonic, then electro-polished with a solution which contains 5g/L $C_{12}H_{25}SO_3Na$ (sodium dodecyl sulfate), 5 g/L KOH and 50 g/L Na_2CO_3 at 20 mA/cm for 1 min. Then the samples were placed immediately in the electrodeposition bath which contains 200 g/L ethylenediammonium dichloride acted as crystal modifier, 30 g/L H_3BO_3 as pH buffer and 200 g/L $NiCl_2 \cdot 6H_2O$ played as ion source, after being washed by water. In the following, the deposition was carried out in a cell, where the platinum wire was used as counter electrode and Ag/AgCl acted as reference electrode. Here, an EG&G computer-controlled galvanostat/potentiostat was connected to the electrochemical cell. A constant current power provided by direct current was used in the stage of electrodeposition for 1, 3 and 5 min respectively, where the current density is around 15 mA/cm^2.

2.2. Surface characterization

According to the sessile drop measurement, contact angle meter (Kyowa Interface Science, DM-501) was used to calculate the water contact angles of the deposited film, where the volume of every water droplet was around 8 μL. Moreover, the tests were carried out at 25^{o}C under air ambient. Five points were recorded to calculate the water contact angles. Field Emission Scanning Electron Microscopy (FE-SEM, Hitachi High-Technology Corp., S-4300) was employed to investigate the surface shape of the super-hydrophobic films, where the accelerating voltage was in the range of 10 to 15 keV. The Mitutoyo surftest (SJ210) roughness profile instrument was utilized to measure the roughness degree of the surface. In addition, X-ray photoelectron spectroscopy was used to analyze the chemical composition of the surface.

2.3. Electrochemical measurements

Unless stated otherwise, all the electrochemical tests were carried out in NaCl water solution (5.0 wt%) at room temperature, where the pH is 6.2. Here the computer-controlled potentiostat was used under the conditions of open circuit. Moreover, the alloy AZ31 coated with Ni film which is super-hydrophobic was employed as the working electrode, whereas a platinum plate was used as the counter electrode. The reference electrode, which was Ag/AgCl, was set in the close vicinity of the circular window. Noted that the AZ31 substrate coated with super-hydrophobic film was dipped in the sodium chloride solution for 30 min, which could promote the system to be stabilized. Subsequently,

in the case of OCP, the potentiodynamic polarization curves were recorded in the range of -400 mV to 800 mV, where the scanning rate is 1 mV/s. Furthermore, the EIS tests were carried out in the frequency range of 0.1 Hz to 100 kHz, where the sinusoidal signal perturbation is 10 mV and five points were recorded after each decade. Noted that every specimen was under immersion for 30 min in prior to the impedance tests. On the base of equivalent electrical analogues, the laboratorial EIS spectra could be illustrated by the program Zplot2.0, so that to gain the proper parameters.

3. RESULT AND DISCUSSION

In this paper, the electrodeposition time was studied as the procedure of the preparation of the Ni coating is essential. The SEM images of the surfaces of various samples collected at diverse times of 0, 1, 3 and 5 min were shown in Figure 1, where it was obvious that the surfaces contained three dimensional microstructures. Moreover, a wide range of bulgy particles, which were uniform and regular, were observed on the samples. It was obvious that the content of bulgy particles increased after 1 min electrodeposition, where an increasing number of particles were arranged on the surface to form the cauliflower-like clusters. As shown in Figure 1C, the surface became significantly rough and was covered by the particles accompanied by the cauliflower-like clusters with a size of 10 to 20 μm, when conducting longer time of electrodeposition. Moreover, it was also shown that small particles with a size of 3 to 4 □m was covered on the surfaces among the particles. As shown in Figure 1D, the particles grew bigger when extending the electrodeposition time, where the Ni coating became thicker.

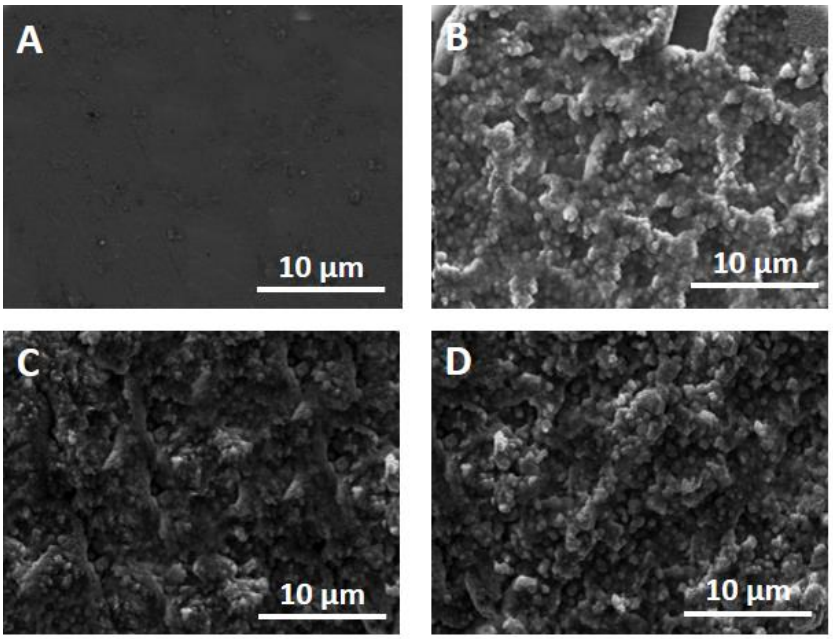

Figure 1. SEM images of the sample surfaces after electrodeposition under the different time at for (A) 0, (B) 1, (C) 3 and (D) 5 min.

The as-prepared coating, which was deposited on the surface of AZ31 Mg alloy, was analyzed by XPS. The XPS spectra of the obtained super-hydrophobic, which had been modified by the stearic acid, was illustrated in Figure 2, where the chemical composition and the contents of C, O, Ni and Mg were calculated. Based on the obtained result, it suggested that Ni coating was the as-prepared coating which was covered on the surface of the AZ31 Mg alloy.

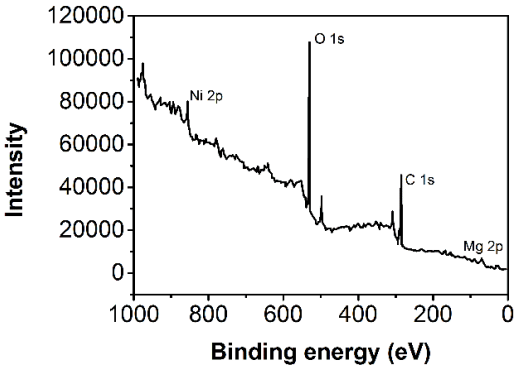

Figure 2. XPS spectrum of the as-prepared super-hydrophobic surface on AZ31 magnesium alloy.

Subsequently, the surface wettability of the deposited film was evaluated by water angle measurements. The relationship between the time of deposition and the water contact angle of the surface film which was covered on Mg alloy AZ31 was illustrated in Figure 3. It was obvious that the water contact angle increased when extending the deposition time. The water contact angle of the surface film, which was hydrophobic, was around 105^{o} when being deposited for 1 min. Conversely, as shown in Figure 3, the surface became super-hydrophobic when the time of deposition was beyond 3 min, where the water contact angle was considerably larger than 150^{o}. Moreover, as illustrated in the FE-SEM and topographic images, it suggested that the static water contact angle was closely positive correlation with the surface roughness of the deposited film. In addition, the electrodeposition time had a significant effect on the wettability. Here, the water contact angle of the surfaces was less than 120^{o} when being electrodeposited for 5 min.

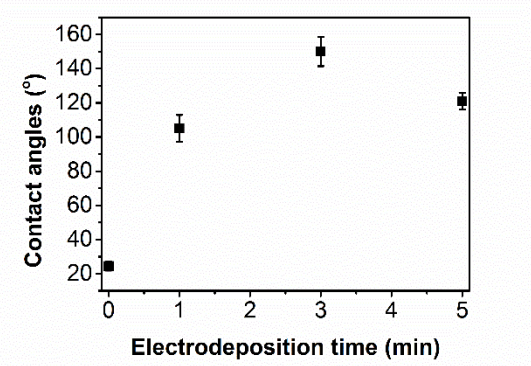

Figure 3. The relationship between water contact angles on the film surface deposited on magnesium alloy AZ31 and the deposition time.

The potentiodynamic polarization curves (Tafel) was used to study the momentary erosion rate. The potentiodynamic poloarization curves of Mg alloy without treatment and the super-hydrophobic surface obtained in NaCl solution (3.5 wt%) was shown in Figure 4, where the Tafel extrapolation method was employed. The data of potentiodynamic polarization measurement was illustrated in Table 1. It was obvious that the erosion potential (Ecoor) of the Mg alloy without treatment (-1.04 V) was lower than that of the obtained super-hydrophobic surface.

The erosion current density (Icorr) of various specimen could be calculated from Tafel curve, based on the potentiodynamic polarization curves linear extrapolation method. Subsequently, based on the equation described below, the corrosion rate *Pi* (mm/y) could be obtained.

$$P_i = 22.85 \times i_{corr}$$

Moreover, the erosion current density (Icorr) of the Mg alloy without treatment was 1.89 × 10^{-3}A/cm^2, whereas that of the obtained super-hydrophobic surface is 5.41 × 10^{-5} A/cm^2. Therefore, the P_i of the specimen (1.23 × 10^{-3} mm/y), which had been electrodeposited with Ni, could be calculated to be 30 times lower than AZ31 without treatment (4.32 × 10^{-2} mm/y). Consequently, these results suggested that the electrodeposition with Ni significantly improved the erosion resistance [45, 46].

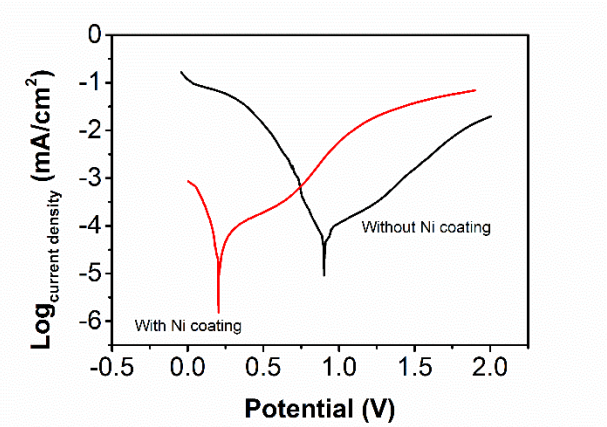

Figure 4. Potentiodynamic polarization curves of the AZ31 magnesium alloy with untreated magnesium alloy and as-prepared super-hydrophobic surface.

Table 1. The results of potentiodynamic polarization test of the AZ31 magnesium alloy, untreated AZ31 and after electrodeposition of nickel in 3.5wt% NaCl solution.

Sample	E_{coor} (V)	Icoor (A/cm^2)
Untreated AZ31	-1.04	1.89 × 10^{-3}
After electrodeposition of nickel	-0.47	5.41 × 10^{-5}

The Nyquist plots was further employed to study the erosion resistances of the obtained super-hydrophobic surface. The Nyquist plots of the AZ31 Mg alloy substrate without any process and the super-hydrophobic obtained in NaCl solution (3.5 wt%) were shown in Figure 5. The results suggested that capacitive loops, which were widely divergent, were caused by the resistance of the charge

transfer during the process of corrosion. Due to surface film of Ni coating which was protective, the capacitive loops of the obtained super-hydrophobic surface had a general tendency compared to the Mg alloy substrate without process.

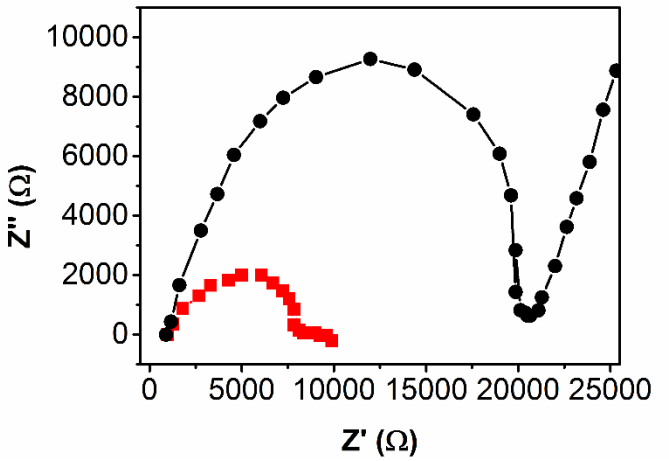

Figure 5. The Nyquist plots obtained from the untreated magnesium alloy substrate, the hydrophobic surface prepared by electroless nickel plating and the super-hydrophobic surface after electrodeposition of nickel and after immersion in 5 wt. % NaCl aqueous solution for 30 min.

Various equivalent circuits were employed to meet with the Nyquist plots, so that to analyze the impedance data precisely. The equivalent circuit patterns of the studied system of AZ 31 sample without treatment and the time constant were shown in Figure 6A. In the analog circuits, the resistance of the solution was illustrated by Rs, where the charge transfer resistance was interpreted in Rct. In addition, the element in immobile phase of the electrical bilayer was represented by CPEdl. Noted that the erosion resistance capacity was analyzed by the value of the Rct. The equivalent ambit patterns of the studied system of the obtained super-hydrophobic surface which was electrodeposited with Ni was shown in Figure 6B, where the capacitance of the surface film was represented by Cc. The impedance of the interface reaction between the substrate and the surface film was illustrated in the Rct||Cdl elements, whereas the the Impedance of interface reaction between the surface film and the electrolytic solution was represented by the parallel combination of Rc and Cc. Moreover, the capacitance and the resistance of air in a tiny stomates was typically represented by the Cari and Rair respectively. The Rair||Cair elements were aligned in parallel to the two elements described above under the consideration of numerous tiny pores which could be filled by air. The optimal results could be gained through applying the equivalent circuit pattern illustrated in Figure 6C to fit the Nyquist plots of the obtained super-hydrophobic surface. It was demonstrated that the Rct value of the super-hydrophobic specimen could reach up to 18051 Ω cm^2, whereas the value of Mg alloy substrate without treatment could only reach 867 Ω cm^2. Thus, it indicated that the coating deposited on the surface had a remarkable effect on promoting the anti-erosion capacity of the Mg alloy. Similar results have been reported by other researchers. For example, Liu and co-workers demonstrated a super-hydrophobic film formed on the copper surface by n-tetradecanoic acid ($CH_3(CH_2)_{12}COOH$) etch and subsequently

show that the corrosion rate of Cu with super-hydrophobic surface decreases dramatically because of its special microstructure [16]. Shen and co-workers reported the formation of a uniform TiO_2 nanoparticle film on the surface of 316L stainless steel by using sol–gel and dip-coating technology [47]. The contact angle of the super-hydrophobic surface is $150 \pm 1°$. It shows, from the electrochemical tests, that the super-hydrophobic coatings on 316L stainless steel exhibit an excellent corrosion resistance in chloride containing solution at the room temperature.

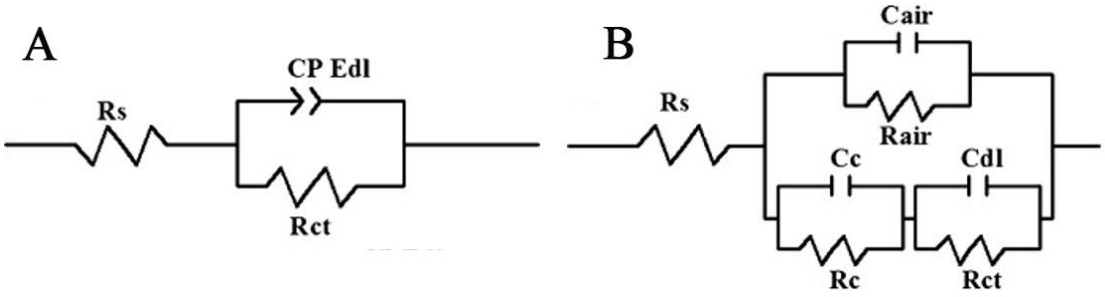

Figure 6. The equivalent circuit models of the studied system: (A) the untreated magnesium alloy substrate and (B) the as-prepared super-hydrophobic surface after electrodeposition of nickel.

4. CONCLUSION

In conclusion, diverse nickel films were fabricated on AZ31 Mg alloy which was not chemically modified through controlling electrodeposition process. Various measurements including optical contact angle meter, scanning electron microscopy, Tafel polarization measurement and electrochemical impedance spectroscopy were utilized to analyze the surface morphology, corrosion resistance and the wettability of the nickel films. According to the results of the potentiodynamic polarization curves (Tafel), it indicates that the corrosion current densities are low, where the results of electrochemical impedance spectroscopy indicate that the obtained super-hydrophobic surface possesses high impedance. Thus, these suggest that Mg alloy could be prevented from erosion by being deposited with the obtained super-hydrophobic film.

ACKNOWLEDGEMENTS
This work was jointly supported by the Ground Plan of Science and Technology Projects of Jiangxi Province, China (Grant No. KJLD2013078) and Open Project of Jiangxi Provincial Engineering Research Center for Magnesium Alloys (2015).

References

1. Z. Yong, J. Zhu, C. Qiu and Y. Liu, *Appl. Surf. Sci.*, 255 (2008) 1672
2. H.-Y. Wang, W. Wang, M. Zha, N. Zheng, Z.-H. Gu, D. Li and Q.-C. Jiang, *Mater. Chem. Phys.*, 108 (2008) 353
3. M.P. Staiger, A.M. Pietak, J. Huadmai and G. Dias, *Biomaterials*, 27 (2006) 1728

4. E. Aghion, B. Bronfin and D. Eliezer, *Journal of Materials Processing Technology*, 117 (2001) 381
5. J. Gray and B. Luan, *J. Alloy. Compd.*, 336 (2002) 88
6. T. Kraus, S.F. Fischerauer, A.C. Hänzi, P.J. Uggowitzer, J.F. Löffler and A.M. Weinberg, *Acta biomaterialia*, 8 (2012) 1230
7. H. Hornberger, S. Virtanen and A. Boccaccini, *Acta biomaterialia*, 8 (2012) 2442
8. F.E.-T. Heakal, A. Fekry and M.A.E.-B. Jibril, *Corrosion Science*, 53 (2011) 1174
9. Y. Song, D. Shan and E. Han, *Mater. Lett.*, 62 (2008) 3276
10. G.-L. Song, *Electrochimica Acta*, 55 (2010) 2258
11. A. Pardo, S. Merino, M. Merino, I. Barroso, M. Mohedano, R. Arrabal and F. Viejo, *Corrosion Science*, 51 (2009) 841
12. O.-U. Nimittrakoolchai and S. Supothina, *Journal of the European Ceramic Society*, 28 (2008) 947
13. F. Zhang, S. Chen, L. Dong, Y. Lei, T. Liu and Y. Yin, *Appl. Surf. Sci.*, 257 (2011) 2587
14. Z. She, Q. Li, Z. Wang, L. Li, F. Chen and J. Zhou, *Chem. Eng. J.*, 228 (2013) 415
15. P. Wang, D. Zhang and R. Qiu, *Corrosion Science*, 54 (2012) 77
16. T. Liu, Y. Yin, S. Chen, X. Chang and S. Cheng, *Electrochimica Acta*, 52 (2007) 3709
17. Y. Wang, W. Wang, L. Zhong, J. Wang, Q. Jiang and X. Guo, *Appl. Surf. Sci.*, 256 (2010) 3837
18. W. Zhang, Z. Yu, Z. Chen and M. Li, *Mater. Lett.*, 67 (2012) 327
19. S. Farhadi, M. Farzaneh and S. Kulinich, *Appl. Surf. Sci.*, 257 (2011) 6264
20. S. Kulinich and M. Farzaneh, *Cold Regions Science and Technology*, 65 (2011) 60
21. L.B. Boinovich, A.M. Emelyanenko, V.K. Ivanov and A.S. Pashinin, *ACS applied materials & interfaces*, 5 (2013) 2549
22. S. Kulinich and M. Farzaneh, *Langmuir*, 25 (2009) 8854
23. W. Xu, X. Shi and S. Lu, *Mater. Chem. Phys.*, 129 (2011) 1042
24. Z. Chen, F. Tian, A. Hu and M. Li, *Surface and Coatings Technology*, 231 (2013) 88
25. Z. Chen, L. Hao, A. Chen, Q. Song and C. Chen, *Electrochimica Acta*, 59 (2012) 168
26. S. Kulinich, S. Farhadi, K. Nose and X. Du, *Langmuir*, 27 (2010) 25
27. A. Satyaprasad, V. Jain and S. Nema, *Appl. Surf. Sci.*, 253 (2007) 5462
28. H. Liu, L. Feng, J. Zhai, L. Jiang and D. Zhu, *Langmuir*, 20 (2004) 5659
29. X. Fan, L. Chen, C. Wong, H.-W. Chu and G. Zhang, *Engineering*, 1 (2015) 384
30. S. Khorsand, K. Raeissi, F. Ashrafizadeh and M. Arenas, *Chem. Eng. J.*, 273 (2015) 638
31. R. Yang, A. Asatekin and K.K. Gleason, *Soft Matter*, 8 (2012) 31
32. R. Lakshmi, T. Bharathidasan, P. Bera and B.J. Basu, *Surface and Coatings Technology*, 206 (2012) 3888
33. N. Ahmad, C. Leo and A. Ahmad, *Appl. Surf. Sci.*, 284 (2013) 556
34. Y. Fan, C. Li, Z. Chen and H. Chen, *Appl. Surf. Sci.*, 258 (2012) 6531
35. A. Nakajima, K. Abe, K. Hashimoto and T. Watanabe, *Thin Solid Films*, 376 (2000) 140
36. T. Hang, A. Hu, H. Ling, M. Li and D. Mao, *Appl. Surf. Sci.*, 256 (2010) 2400
37. W. Xi, Z. Qiao, C. Zhu, A. Jia and M. Li, *Appl. Surf. Sci.*, 255 (2009) 4836
38. C. Spathi, N. Young, J.Y. Heng, L.J. Vandeperre and C.R. Cheeseman, *Mater. Lett.*, 142 (2015) 80
39. A.M. Atta, G.A. El-Mahdy, H.A. Allohedan and S.M. El-Saeed, *Int. J. Electrochem. Sci*, 10 (2015) 8
40. N. Soltani and M. Khayatkashani, *Int. J. Electrochem. Sc.*, 10 (2015) 46
41. G. Wang and T.-Y. Zhang, *Journal of colloid and interface science*, 377 (2012) 438
42. W. Geng, A. Hu and M. Li, *Appl. Surf. Sci.*, 263 (2012) 821
43. M. Guo, Z. Kang, W. Li and J. Zhang, *Surface and Coatings Technology*, 239 (2014) 227
44. Y. Wang, J. Xue, Q. Wang, Q. Chen and J. Ding, *ACS applied materials & interfaces*, 5 (2013) 3370

45. A. Pardo, M. Merino, A.E. Coy, R. Arrabal, F. Viejo and E. Matykina, *Corrosion Science*, 50 (2008) 823
46. M.B. Kannan and V. Raja, *Metallurgical and Materials Transactions A*, 38 (2007) 2843
47. G.X. Shen, Y.C. Chen, L. Lin, C.J. Lin and D. Scantlebury, *Electrochimica Acta*, 50 (2005) 5083